Eur Biophys J (2010) 39:855–860
DOI 10.1007/s00249-009-0508-z

BIOPHYSICS LETTER

Confined detection volume of fluorescence correlation spectroscopy by bare fiber probes

Guowei Lu · Franck H. Lei · Jean-François Angiboust · Michel Manfait

Received: 19 March 2009 / Revised: 28 May 2009 / Accepted: 10 June 2009 / Published online: 3 July 2009

Abstract A fiber-tip-based near-field fluorescence correlation spectroscopy (FCS) has been developed for confining the detection volume to sub-diffraction-limited dimensions. This near-field FCS is based on near-field illumination by coupling a scanning near-field optical microscope (SNOM) to a conventional confocal FCS. Single-molecule FCS analysis at 100 nM Rhodamine 6G has been achieved by using bare chemically etched, tapered fiber tips. The detection volume under control of the SNOM system has been reduced over one order of magnitude compared to that of the conventional confocal FCS. Related factors influencing the near-field FCS performance are investigated and discussed in detail. In this proof-of-principle study, the preliminary experimental results suggest that the fiber-tip-based near-field FCS might be a good alternative to realize localized analysis at the single-molecule level.

Keywords Fluorescence correlation spectroscopy · Scanning near-field optical microscopy · Tapered fiber tips · Detection volume

Electronic supplementary material The online version of this article (doi:10.1007/s00249-009-0508-z) contains supplementary material, which is available to authorized users.

G. Lu · F. H. Lei · J.-F. Angiboust · M. Manfait
Unité MéDIAN, UFR Pharmacie, Université de Reims Champagne-Ardenne, UMR CNRS 6237, 51 rue Cognacq-Jay, 51096 Reims Cedex, France

G. Lu (✉)
State Key Laboratory for Mesoscopic Physics, Department of Physics, Peking University, 100871 Beijing, China
e-mail: guowei.lu@univ-reims.fr

Fluorescence correlation spectroscopy (FCS) is a powerful tool for characterizing dynamic behaviors and kinetic properties of biochemical reactions in vitro and in vivo (Rigler et al. 1993). At present most FCS instruments are based on confocal optics for confining the detection volume, typically to 250 attoliters (al). Such a tiny sampling volume requires a fluorophore concentration in the nanomolar range to isolate individual molecules. However, many reactions in biology and biochemistry demand measurements at micromolar concentrations. Hence, in order to realize single-molecule measurements, the sampling volume needs to be further reduced. In the last decade, great progress in restricting the FCS sampling volume has been made. For instance, two-photon excitation FCS achieved detection volumes as small as about 100 al with good signal-to-noise ratio despite some experimental difficulties (Berland et al. 1995). The FCS detection volume by stimulated emission depletion (STED) technique allowed fivefold reduction over the diffraction-limited one (Kastrup et al. 2005). Micro-channels in fused silica confined sampling volumes to about 2 al (Foquet et al. 2004). Taking advantage of the total internal reflection (TIR), optical evanescent field illumination FCS allowed a detection volume 10 times smaller than those of the conventional FCS (Ruckstuhl and Seeger 2004).

However, reducing the sampling volume further seems to be difficult to realize with far-field optics and has become a real challenge. Levene et al. were the first to introduce nano-holes to FCS measurements and several groups followed (Levene et al. 2003; Rigneault et al. 2005; Wenger et al. 2005). These authors deposited a thin metal film with nanoscale holes on a coverslip to restrict the FCS sampling volume to zeptoliters. The FCS analysis of high concentration solutions was accomplished in one nano-hole serving as zero-mode waveguide. But the method requires

the molecules of interest to enter into the nano-hole for the FCS measurements, which limits its applications in biophysical research in some ways (Samiee et al. 2006). On the other hand, optical probes used in scanning near-field optical microscopy (SNOM) can offer an illuminating source with subdiffraction diameters. In addition, SNOM also allows imaging the sample surface topographically. Up to now, few investigations concerning the integration of SNOM and FCS have been reported. Recently, a special SNOM probe with 3.65-μm-diameter aperture was used by Lewis et al. for FCS measurement of 100 nM Rhodamine 6G (R6G) molecules (Lewis et al. 2007). In their study, the long diffusion time of FCS (a few milliseconds) was attributed to the large light beam from such a probe. Our results show that molecular surface adsorption also greatly influences the diffusion time of FCS measurements except for the field distribution of excitation light (Lu et al. 2008; "Supplemental material").

As in any scanning probe microscopy, one of the key elements of the SNOM–FCS system is the probe tip. Undoubtedly, metal-coated, tapered fiber tip with sub-wavelength aperture can provide a sub-diffraction excitation volume smaller than the conventional confocal microscope. But it is still difficult to obtain the sub-diffraction-limited detection volume from the $G(0)$ value of FCS measurements because of unexpected noise background (Vobornik et al. 2008; "Supplemental material"). And some disadvantages of metal-coated probes still repress the intrinsic advantages of integrating SNOM and FCS, such as low-light throughput efficiency, instability of the metal-coated layer, complicated fabrication process, and high cost. In this study, the bare, chemically etched, tapered optical fiber tips were used directly as the SNOM probe for near-field FCS measurements. The field distribution of the excitation light from this probe and measurement performance of integrating SNOM and FCS were investigated and are discussed in detail.

The developed SNOM–FCS set-up shown schematically in Fig. 1 is a home-built system attached to an inverted optical microscope (Olympus IX-70, Japan); it was described previously in detail (Lu et al. 2008; Lei et al. 2006). In brief, the laser beam from an argon ion laser emitting at 488 nm is filtered with a laser line filter (488 nm, MaxLine Laser-line filter) and then coupled (F-916 coupler, Newport, USA) into an optical fiber. This fiber tip is fixed onto a piezoelectric bimorph lever serving as the force sensor of the SNOM. The fluorescent signal excited by the light diffused from the fiber tip is collected with a water immersion objective lens (NA = 1.2, 60×, UplanApo, Olympus), filtered by a narrow band-pass filter (556/20 nm, Semrock), and then focused onto a multimode fiber with 12-μm core diameter serving also as a pinhole. Finally, the fluorescence signal is guided to a single-photon

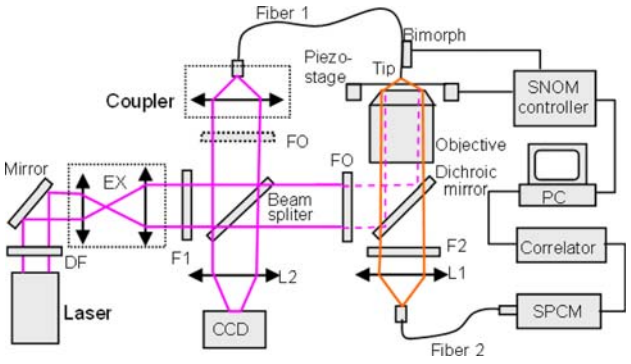

Fig. 1 Diagram of the FCS/SNOM experimental set-up based on fiber-tip illumination. *EX* Telescope beam expander, *F1* laser line filter, *F2* band-pass filter, *FC* fiber coupler, *FO* flip opaque plate, *L1* aspheric lens, *D1* dichroic mirror, *BS* beam splitter, *Fiber 1* single-mode fiber with aluminum-coated tip, *Fiber 2* multimode fiber

counting module (SPCM-AQR-14-FC, PerkinElmer) and is then fed into a digital correlator (Flex02-12D, Correlator.com). The system can operate in either the fiber tip illuminating near-field FCS mode or the conventional confocal FCS mode, depending on the position of the flip opaque plate. Signal acquisitions are carried out on a droplet of R6G (about 10 or 100 nM) in Tris-buffered saline solution with Tween-20. In order to obtain a super-hydrophilic surface that can completely avoid molecule adsorption onto the surfaces, the microscope coverslip and the fiber tips are both treated with oxygen plasma technique (Femto3, Diener, Germany) for 5 min before being used in the FCS measurements. Details concerning the influence of the dye-adsorbed surface on FCS measurements are given in the "Supplemental material."

For comparison, the optical fiber with cleaved end was used firstly to perform FCS measurements on account of manufacturing simplicity, known light field distribution, and high light throughput efficiency. At the beginning, the cleaved fiber end was positioned about 100 μm above the coverslip surface. The focal plane of the objective lens was adjusted through the focus knob of the optical microscope close to the fiber end to collect the fluorescence signals excited by the cleaved fiber end. Several kinds of optical fibers, such as single-mode fibers at wavelength 488 nm (SM450, S405, and S460, Thorlabs) and multimode fibers (SM600, SMF28, AFS50/125Y, and AFS105/125Y, Thorlabs) were utilized for comparing their characteristics. The results show that the excitation light field distribution of the single-mode fibers is more suitable for a feasible FCS performance. And the single-mode fibers with pure silica core, such as S405 and S460, show less fluorescent background and the best signal-to-noise ratio, while the multimode fibers for FCS measurements do not work well because of their complex output field distribution. Generally, one can still observe the FCS signal by a cleaved

multimode fiber end with smaller core diameter (data not shown here). The FCS auto-correlation could no longer be observed when the cleaved fiber end was made from multiple mode fibers with a core over 50 μm in diameter.

Typical auto-correlation curves for the R6G solution in Tris buffer excited by the cleaved fiber end made from single-mode fiber S405 are shown in Fig. 2. Three FCS curves measured at different distances between the objective focal plane and the fiber end apex are presented. The shape variation of the FCS curves at different points should be attributed mainly to the difference in light field distribution profile $I(r)$. The axial extent of $I(r)$ is over 50 μm where the FCS auto-correlation signal can be clearly observed by adjusting the objective lens along the axial direction of the fiber tips. As shown in Fig. 2, the FCS curves closer to the fiber end show shorter diffusion times and higher $G(0)$ values, meaning that the lateral extension of the excitation field and detection volume is smaller near the fiber end. The fitting curves by the standard 3D Gaussian model are presented in Fig. 2 (Wenger et al. 2005; Leutenegger et al. 2006). The diffusion times are about 210 ± 5, 270 ± 10, and 310 ± 30 μs at points (a) (very close to the surface of fiber end), (b) [10 μm away from point (a)], and (c) [20 μm away from the point (a)], respectively. Thus, at the front of the fiber-end surface, the lateral excitation full width ω_0 at points (a), (b), and (c) was about 485, 550, and 590 nm, respectively, according to the equation $\tau = r^2/4D$ where the diffusion time is about 50 μs and lateral width is about 240 nm for the conventional confocal FCS. The mean half divergence angle was estimated to be about 0.15°. The results are consistent with the fact that the field intensity distribution emitted from the

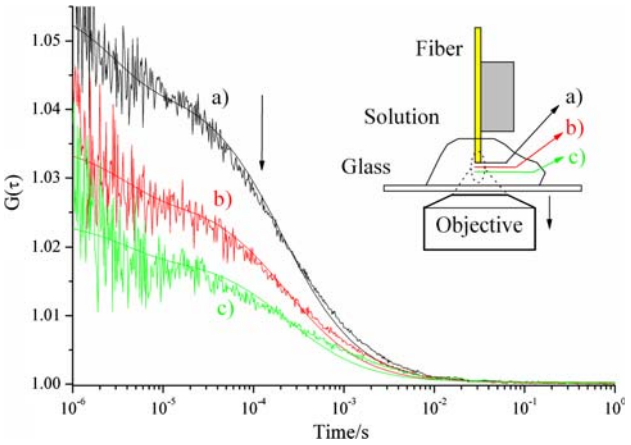

Fig. 2 The rough curves are typical original auto-correlation data excited by a cleaved fiber end for R6G (10 nM) molecules in Tris buffer and collected by the objective lens at different positions: *(a)* very close to the fiber end surface, *(b)* about 10 μm from point *(a)*, and *(c)* about 20 μm from point *(a)*. The *solid smooth lines* are fitted curves. *Inset* shows the FCS schematically with illumination by a cleaved fiber end

cleaved single-mode fiber end is very similar to a Gaussian beam with a small divergence angle, and the beam waist locates at the fiber end surface (Marcuse 1978). The light field distribution is reliable compared to the conventional simulation of the single-model fiber. Interestingly, the FCS diffusion time near the cleaved end is almost one order of magnitude smaller than that of the special SNOM probe (Lewis et al. 2007), which means that the influence of molecular surface adsorption on FCS measurements should be considered in this situation.

The $G(0)$ value obtained by the cleaved fiber illumination is certainly smaller than that excited by the objective lens for the same R6G solution, since it is obvious that the excitation volume of the cleaved fiber tip is larger than that of the conventional confocal FCS. For instance, the detection volume for point (a) in Fig. 2 is larger by nearly a factor of 8 compared to the conventional objective lens, including about fourfold expansion in lateral extension and about twofold stretching in the axial direction (here, the influence of background noise has not been taken into account). It should also be noted that the 3D-Gaussian beam shape of the simulation model is just used as an approximation, but its results are fortunately acceptable. Meanwhile, the FCS detection volume illuminated by the cleaved fiber end can be reduced further by bringing the fiber end in the vicinity of the coverslip surface under control of the SNOM system. The SNOM–FCS measurement results show that a small channel between the fiber end and the coverslip usually leads to 1.5- to 3-fold increase in the $G(0)$ value, which means that the detection volume is decreased by the confinement effect. The shear force mechanism is able to control the distance at 20–30 nm between the fiber end and the coverslip surface. However, in most cases the plane of the fiber end (125 μm in diameter, not perfectly planar, but rather with some kind of protrusion) can not be adjusted to be completely parallel to the coverslip surface plane, and the optical beam with about 1 μm in diameter at the fiber-end surface is larger than the diffraction-limited one of the objective lens. All these limit the confinement effect of the FCS detection volume. A better confinement of detection volume can be achieved by a bare chemically etched tapered fiber tip, as discussed in detail in the following paragraph because it possesses a sharper tip and more tightly focused excitation light field.

The bare chemically etched tapered fiber tip is fabricated by the common chemical-etching or tube-etching methods. In brief, striped or nonstriped S405 or S460 fiber is immersed in 48% aqueous hydrofluoric acid covered with an organic protection layer. This results in a tapered tip in an auto-stopping process after about 40 min for common chemical etching or after about 120 min for tube etching. Their typical images are shown in the inset of

Fig. 3. Firstly, the chemically etched bare fiber tip is positioned about 100 μm above the coverslip surface. The FCS measurements excited with such tips are performed at different positions by adjusting the objective lens focal plane in the axial direction. Three typical FCS curves for 10 nM R6G solution at different positions with an etched tip made from single-mode fiber S460 are shown in Fig. 3. Point (a) is very close to the tip apex, point (b) is about 3 μm away from point (a), and point (c) is about 6 μm from point (a). Here, the position of point (a) is roughly estimated by the size of the light spot and accurately determined by the fluorescence intensity because the highest excitation field intensity is near the tip apex. The standard 3D Gaussian model fits well the FCS curves, and the fitting curves are shown in Fig. 3 with corresponding color. The diffusion times of these three points are about 40 ± 2, 120 ± 5, and 240 ± 30 μs for points (a), (b) and (c), respectively. The lateral widths ω_0 of the excitation field at these three points are estimated to be about 215, 370, and 520 nm according to the equation $\tau = r^2/4D$, respectively. And the mean half divergence angle of the excitation field is about 1.46°, which is about one order lager than that of the cleaved fiber end. Obviously, the optical field distribution of the bare chemically etched fiber tip is different from the cleaved fiber end, that is, the etched fiber tip has a smaller waist size and larger divergence angle. Unlike the cleaved fiber end, the FCS auto-correlation signal for the chemically etched fiber tips can be observed only within a smaller range along the axial direction, typically less than 15 μm in front of the tip apex.

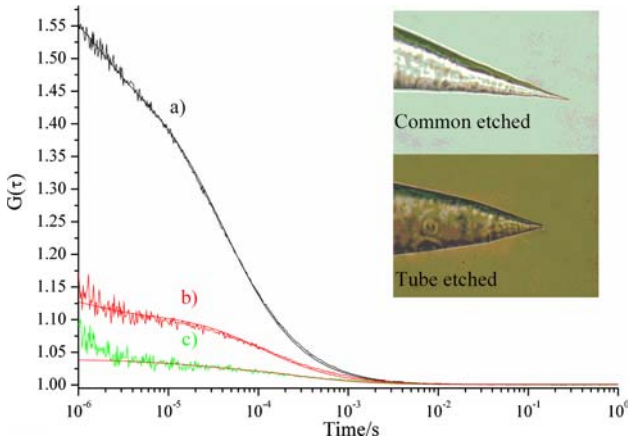

Fig. 3 The rough curves are typical original FCS auto-correlation data excited by a chemically etched fiber tip for R6G molecules (~10 nM) in Tris buffer, and collected by the objective lens at different positions: *(a)* very close the fiber tip apex surface, *(b)* about 3 μm from the point *(a)*, and *(c)* about 6 μm from the point *(a)*. The *solid smooth lines* are fitted curves. *Inset pictures* show typical optical microscopy images of two fiber tips prepared, respectively, by the common chemical-etching method and the tube-etching method

Interestingly, near the tapered etched-tip apex, the field extension (diffusion time about 40 μs and lateral width about 215 nm) is even smaller than the diffraction limit by the objective lens with N.A. 1.2 (diffusion time about 50 μs and lateral width about 240 nm). The smaller field extension of bare tapered tips also results in a smaller detection volume, which is indicated by the $G(0)$ value of point (a) in Fig. 3. The detection volume decreases about 25% compared to that excited by the conventional objective lens, including about 80% (40/50 μs) contribution from reduced lateral extension. And one may conclude that the axial range of the light field of the bare tapered tip is about 20% shorter than the objective lens. This result is the experimental evidence that the chemically etched bare fiber tip can provide a tightly focused light spot close to the diffraction-limited one. For comparison, a bare fiber tip made by the pulling technique was utilized for FCS measurements. The signal-to-noise ratio was very poor because most of the light leaked out from the sides of the probe rather than being emitted from the tip apex.

Since only one bare pulled fiber tip was tested, it is hard to conclude that bare pulled fiber tip is not suitable for such an illumination scheme. Nevertheless, the micro-structure of the pulled fiber tip apex is very complex and the inner core does not remain at the tip apex (Garcia-Parajo et al. 1995), apparent disadvantages compared to chemically etched fiber tips. The apex radius of the latter depends on the etching process, in particular on the time of chemical etching. For the common etching method, the results show that the tips etched for 35–60 min have almost the same FCS diffusion times, which indicates their similar field extension. The field extension would increase with the tips etched for longer etching times, since the tip apex radius could become larger.

According to all of the results above, the FCS measurements provide a good way to estimate the excitation field distribution at the nano-scale. The molecule detection efficiency can be simulated or fitted from the FCS original curves, then the excitation field intensity distribution $I(r)$ is separated from molecule detection efficiency by dividing out the collection efficiency function of the optical system. It follows that FCS could be a useful tool to measure the field distribution at the nano-scale level, although that is beyond the scope of this study.

Furthermore, the FCS detection volume of the chemically etched tapered fiber tip can be reduced further under control of the SNOM system. As is known in scanning probe microscopy, the tip-sample distance can be controlled within 20–30 nm by shear force detection. Consequently, the axial extension would be reduced by more than a factor of 30 resulting in smaller detection volumes when the etched tip apex is in the vicinity of the glass surface (assuming the axial dimension is ~700 nm). As shown in

the inset (a) in Fig. 4, the detection volume is confined between the tip and the glass surface. Typical results for 100 nM R6G solution are shown in Fig. 4, in which curve (a) is the FCS auto-correlation when the tip is near the surface, and curve (b) is the FCS auto-correlation when the tip is removed from the glass surface by about 30 μm. The positions of the tip and the objective focal plane are always fixed, and the glass fixed on the 3D piezo-stage is auto-active under SNOM shear force control. The results show that the diffusion times in both situations are the same, but the value of $G(0)$ goes up by a factor of about 12-fold when the bare tip is positioned near the glass surface. Moreover, because of the light leaking from the bare tip side, the actual detection volume is larger than the confinement gap volume. And, assuming that the fiber's auto-fluorescence background is the same in both situations, this background and the leaking light should compensate for the deviation between the experimental measurements and the rough geometrical estimation of the detection volume. Since the FCS detection volume excited by the bare tapered tips is already smaller than that of the objective lens in far field situation, it is obvious that the detection volume confined between the bare tapered tip and the coverslip surface is more than an order of magnitude smaller than that of the conventional confocal FCS.

Moreover, the etched tapered fiber tip is a suitable probe for obtaining topographic images of the scanned surface. The inset of Fig. 4 shows a typical 60 × 60 μm surface image with resolution of 256 × 256 pixels scanned by a bare fiber probe on the coverslip surface. Some dust adsorbing on the glass surface is present. It is feasible to place the etched tip-source at any point of interest for FCS measurements after the SNOM topographic or optical images have been obtained—a technique that is still under development. And it is worth noting that an intact bare-tip apex is more critical for FCS measurements than for surface imaging. A glass surface covered with a soft biological layer (e.g., lipid bilayer) could reduce tip apex damage during scanning. It was found that the bare tapered tips prepared by the tube-etching method were less fragile than those made by the common chemical-etching method. The tube-etched tip apex is mechanically firmer because of its larger tapered angle as shown in the inset of Fig. 3, while the FCS curves obtained with the tube-etched tip are similar to those of the tips made by the common etching method. Also the FCS measurements with bare tapered tips show as good a signal-to-noise ratio as the conventional confocal FCS. Therefore, chemically etched fiber tips have their advantages compared to metal-coated probes, such as low cost, availability, reliable reproducibility, high light transmittance efficiency, and sharp tip apex (Stockle et al. 1999). Thus, the chemically etched fiber is a good choice to perform SNOM–FCS.

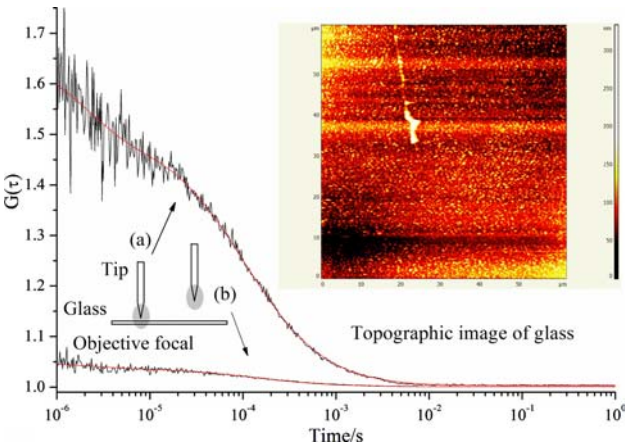

Fig. 4 The rough curves are typical original auto-correlation data excited by the chemically etched fiber tip for R6G molecules (about 100 nM) in Tris buffer and collected by the objective lens near the tip apex. For curve *(a)*, the tip apex is positioned about 20 nm above the coverslip surface under the control of the SNOM system, and for *(b)* the tip apex is positioned about 30 μm above the coverslip surface. The *solid smooth lines* are fitted curves. *Inset pictures* show the chemically etched fiber tip illumination SNOM–FCS schematically and typical topographic images of glass coverslip

In summary, a single-molecule spectroscopy system was successfully established by combining SNOM and FCS techniques. FCS measurements of 100 nM R6G at the single-molecule level were achieved by using bare chemically etched tapered fiber tips, leading to a decrease in the detection volume by over one order of magnitude compared to the conventional confocal FCS. Topographic imaging and FCS spectroscopy of a sample can be obtained simultaneously by the SNOM–FCS system. The bare tube chemically etched fiber tip presented the best performance with high signal-to-noise ratio characteristic both of FCS measurements and stable topographic imaging of SNOM. The preliminary results have shown that the near-field FCS using the bare tapered fiber tip is a promising alternative to perform localized single-molecule-level analysis with high spatial resolution.

Acknowledgments This research was supported by the Conseil Régional Champagne-Ardenne (Convention: 7P06 and 7P07), France.

References

Berland KM, So PTC, Gratton E (1995) Two-photon fluorescence correlation spectroscopy: method and application to the intracellular environment. Biophys J 68:694

Foquet M, Korlach J, Zipfel WR, Webb WW, Craighead HG (2004) Focal volume confinement by submicrometer size fluidic channels. Anal Chem 76:1618

Garcia-Parajo M, Tate T, Chen Y (1995) Gold coated parabolic tapers for scanning near-field optical microscopy: fabrication and optimization. Ultramicroscopy 61:155

Kastrup L, Blom H, Eggeling C, Hell SW (2005) Fluorescence fluctuation spectroscopy in subdiffraction focal volumes. Phys Rev Lett 94:178104

Lei FH, Huang H, Piot O, Trussardi A, Manfait M, Shang G, Troyon M (2006) Active bimorph-based tapping-mode distance for scanning near-field optical microscopy of biological samples in liquid. J Appl Phys 100:84317

Leutenegger M, Gosch M, Perentes A, Hoffmann P, Martin OJF, Lasser T (2006) Confining the sampling volume for fluorescence correlation spectroscopy using a sub-wavelength sized aperture. Opt Express 14:956

Levene MJ, Korlach J, Turner SW, Foquet M, Craighead HG, Webb WW (2003) Zero-mode waveguides for single-molecule analysis at high concentrations. Science 299:682

Lewis A, Kuttner YY, Dekhter R, Polhan M (2007) Fluorescence correlation spectroscopy at 100 nM concentrations using near-field scanning optical microscopic geometries and highly diffracting force sensing fiber probes. Isr J Chem 47:171

Lu GW, Lei FH, Angiboust JF, Roche Y, Huang LY, Manfait M (2008) Near-field fluorescence correlation spectroscopy by using a tapered optical fiber tip as excitation source. In: Bubendorff JL, Lei FH (eds) Advanced technologies and applications on scanning probe microscopy. Research Signpost, Trivandrum, India, pp 89–100

Marcuse D (1978) Gaussian approximation of the fundamental modes of graded index fibers. J Opt Soc Am 68:103

Rigler R, Mets U, Widengren J, Kask P (1993) Fluorescence correlation spectroscopy with high count rate and low background—analysis of translational diffusion. Eur Biophys J 22:169

Rigneault H, Capoulade J, Dintinger J, Wenger J, Bonod N, Popov E, Ebbesen TW, Lenne P-F (2005) Enhancement of single-molecule fluorescence detection in subwavelength apertures. Phys Rev Lett 95:117401

Ruckstuhl T, Seeger S (2004) Attoliter detection volumes by confocal total-internal-reflection fluorescence microscopy. Opt Lett 29:569

Samiee KT, Moran-Mirabal JM, Cheung YK, Graighead HG (2006) Zero mode waveguides for single molecule spectroscopy on lipid membranes. Biophys J 90:3288

Stockle R, Fokas C, Deckert V, Zenobi R, Sick B, Hecht B, Wild UP (1999) High quality near field optical probes by tube etching. Appl Phys Lett 75:160

Vobornik D, Banks DS, Lu Z, Fradin C, Taylor R, Johnston LJ (2008) Fluorescence correlation spectroscopy with subdiffraction-limited resolution using near-field optical probes. Appl Phys Lett 93:163904

Wenger J, Lenne P-F, Popov E, Rigneault H, Dintinger J, Ebbesen TW (2005) Single molecule fluorescence in rectangular nano-apertures. Opt Express 13:7035